

# EVI1 carboxy-terminal phosphorylation is ATM-mediated and sustains transcriptional modulation and self-renewal via enhanced CtBP1 association

Roberto Paredes<sup>1,2,†</sup>, Marion Schneider<sup>1,2,†</sup>, Adam Stevens<sup>2,3</sup>, Daniel J. White<sup>1,2</sup>, Andrew J.K. Williamson<sup>1,2</sup>, Joanne Muter<sup>1,2</sup>, Stella Pearson<sup>1,2</sup>, James R. Kelly<sup>1,2</sup>, Kathleen Connors<sup>1,2</sup>, Daniel H. Wiseman<sup>2,4</sup>, John A. Chadwick<sup>2,4</sup>, Harald Löffler<sup>5</sup>, Hsiang Ying Teng<sup>1,2</sup>, Simon Lovell<sup>2,6</sup>, Richard Unwin<sup>1,2</sup>, Henri J. van de Vrugt<sup>7</sup>, Helen Smith<sup>2,6</sup>, Olga Kustikova<sup>8</sup>, Axel Schambach<sup>8</sup>, Tim C.P. Somerville<sup>2,4</sup>, Andrew Pierce<sup>1,2</sup>, Anthony D. Whetton<sup>1,2,9</sup> and Stefan Meyer<sup>1,2,10,11,\*</sup>

<sup>1</sup>Stem Cell and Leukaemia Proteomics Laboratory, Division of Cancer Sciences, Faculty of Biology, Medicine and Health, University of Manchester, Palatine Road, Manchester M20 3LI, UK, <sup>2</sup>Manchester Academic Health Science Centre, Manchester, UK, <sup>3</sup>Division of Developmental Biology and Medicine, Faculty of Biology, Medicine and Health M13 9WL, University of Manchester, UK, <sup>4</sup>Leukaemia Biology Group, CRUK Manchester Institute, Manchester M20 4XB, UK, <sup>5</sup>Clinical Cooperation Unit Molecular Hematology/Oncology, German Cancer Research Center (DKFZ) and Department of Internal Medicine V, University of Heidelberg, Heidelberg, Germany, <sup>6</sup>Evolution, Systems and Genomics Domain, Faculty of Biology, Medicine and Health, University of Manchester, Manchester M13 9PT, UK, <sup>7</sup>Oncogenetics, Department of Clinical Genetics, VU University Medical Center, Amsterdam, The Netherlands, <sup>8</sup>Institute of Experimental Hematology, Hannover Medical School; Hannover, Germany, <sup>9</sup>Stoller Biomarker Discovery Centre, University of Manchester, Manchester M13 9NQ, UK, <sup>10</sup>Department of Paediatric Haematology and Oncology, Royal Manchester Children's Hospital, Manchester M13 9WL, UK and <sup>11</sup>Young Oncology Unit, The Christie NHS Foundation Trust, Manchester M20 4XB, UK

Received February 07, 2018; Revised May 24, 2018; Editorial Decision May 26, 2018; Accepted May 29, 2018

## ABSTRACT

The transcriptional regulator EVI1 has an essential role in early hematopoiesis and development. However, aberrantly high expression of *EVI1* has potent oncogenic properties and confers poor prognosis and chemo-resistance in leukemia and solid tumors. To investigate to what extent EVI1 function might be regulated by post-translational modifications we carried out mass spectrometry- and antibody-based analyses and uncovered an ATM-mediated double phosphorylation of EVI1 at the carboxy-terminal S858/S860 SQS motif. In the presence of genotoxic stress EVI1-WT (SQS), but not site mutated EVI1-AQA was able to maintain transcriptional patterns

and transformation potency, while under standard conditions carboxy-terminal mutation had no effect. Maintenance of hematopoietic progenitor cell clonogenic potential was profoundly impaired with EVI1-AQA compared with EVI1-WT, in particular in the presence of genotoxic stress. Exploring mechanistic events underlying these observations, we showed that after genotoxic stress EVI1-WT, but not EVI1-AQA increased its level of association with its functionally essential interaction partner CtBP1, implying a role for ATM in regulating EVI1 protein interactions via phosphorylation. This aspect of EVI1 regulation is therapeutically relevant, as chemotherapy-induced genotoxicity might detrimentally sustain EVI1 func-

\*To whom correspondence should be addressed. Tel: +44 161 446 3090; Fax: +44 161 446 3091; Email: stefan.meyer@manchester.ac.uk

†The authors wish it to be known that, in their opinion, the first two authors should be regarded as Joint First Authors.

Present addresses:

Richard Unwin, Division of Cardiovascular Sciences, School of Medical Sciences, Faculty of Biology, Medicine and Health, University of Manchester, Manchester, UK.

Harald Löffler, Zentrum für Innere Medizin III, Marienhospital, Stuttgart, Germany.

## tion via stress response mediated phosphorylation, and ATM-inhibition might be of specific targeted benefit in EVI1-overexpressing malignancies.

### INTRODUCTION

EVI1 is a transcriptional regulator with an essential role in early development and hematopoiesis (1–3). However, aberrantly high expression of *EVII*, which frequently results from chromosomal aberrations involving MECOM (MDS-EVI1 complex) locus on 3q26, where *EVII* is encoded, has potent oncogenic properties with transformation capabilities *in vivo* and *in vitro* (4,5). In acute myeloid leukemia (AML) high *EVII* expression is associated with poor response to cytotoxic treatment and adverse outcome (6,7). *EVII* overexpression has been linked to leukemic transformation in children undergoing gene therapy (8), and individuals affected by Fanconi Anaemia (FA), which is an inherited DNA damage response defect with cancer predisposition (9,10). High *EVII* expression conferring resistance to cytotoxic treatment and poor prognosis is also seen in other malignancies (11–14). Modulation of transcription by EVI1 is not understood in detail, and might, as for other transcriptional regulators, be partly dependent on the cell context of the *EVII* overexpression event (15,16). Thus, *EVII*-coregulated genes are variable in different types of leukemia (17), but nonetheless transcriptional patterns mediated by EVI1 in AML are enriched for genes involved in metabolic processes, differentiation and proliferation, and affect metabolic dependence on mitochondrial creatine kinase (18,19). Several transcripts are encoded in the MECOM locus, of which the main transcript encodes the 145 kDa EVI1 nuclear protein, which consists of an N-terminal zinc finger domain with seven motifs, a proline rich central repressor domain, a smaller C-terminal zinc finger domain with three motifs, and a carboxyterminal acidic domain. EVI1 modulates transcription by direct interaction of its zinc fingers with specific DNA sequences (20,21), and also via recruitment of other transcriptional regulators and chromatin modelling factors (22–25), which promotes the concept of EVI1 as a mediator of epigenetic changes that maintain a stem cell like phenotype with transforming capability (3). Specifically, the interaction of EVI1 with the co-repressor C-terminal binding protein 1 (CtBP1) has been shown to be essential for EVI1-mediated transformation (26,27). As post-translational modifications of EVI1 have been implicated in modulation of transforming ability and EVI1 protein interactions (28,29), we further investigated the role of phosphorylation in modulating EVI1 function. We report here on carboxy-terminal phosphorylation in response to genotoxic stress and associated consequences for EVI1 function. These define an opportunity for ameliorating treatment of diseases associated with EVI1 overexpression by targeting ATM kinase.

### MATERIALS AND METHODS

#### Cell lines and tissue culture

The FA-derived AML cell line SB1690CB, which expresses high levels of EVI1, and the EVI1 negative AML cell line

OCI-AML5 were maintained as described previously (10). HEK293T cells and Rat1 fibroblasts were used as previously described (28). Genotoxic stress was induced by treatment with H<sub>2</sub>O<sub>2</sub> at concentrations previously used (30), or irradiation using a 320 kV X-ray system (Gulmay Medical Ltd) for suspension culture leukemia cells or using the image-guided micro-irradiation system for 96 well plates provided via the SARRP research platform (Xstrahl). Induction of activation of the DNA damage response was confirmed by demonstration of increased quantities of  $\gamma$ H2AX foci and p53 phosphorylation. ATM inhibition was achieved with pretreatment for 1 h in the presence of 10  $\mu$ M of the ATM-inhibitor KU55933 (Torcis).

#### Antibodies

For detection of human EVI1 a polyclonal antibody raised against the N-terminal EVI1 epitope MKSEDPHETMAPDI (Eurogentec), and the EVI1 antibodies #2265 and #2593 (Cell Signaling Technology, CST) were used. For detection of phosphorylated EVI1 we used phospho-specific, affinity purified rabbit polyclonal antibodies raised against EVI1-phospho-peptides NSNHGSQpSPRNVEC for serine 860 (S860) phosphorylation (anti-pS860-EVI1), and NSNHGpSQpSPRNVEC for serine 858 and serine 860 (S858/S860) double phosphorylation (anti-pS858/pS860-EVI1) (Eurogentec) (further details Supplementary Figure S1). For other antibodies see Supplementary Material Table S1.

#### Immunoprecipitation, co-immunoprecipitation and western Blot

Cell lysis and immunoprecipitation were carried out as previously described (28). EVI1 was immunoprecipitated with EVI1 antibody #2593 (Cell Signaling) and captured with protein A sepharose beads. For immunoprecipitation of flag-tagged proteins transfected cells were incubated for one hour with FlagM2 magnetic beads (Sigma). Protein electrophoresis and western blots were carried out using standard methodologies (28). For quantitation of non-saturated western blot signals see Supplementary Methods and Supplementary Figure S2.

#### Mass spectrometry

Immunoprecipitated EVI1 from  $6 \times 10^8$  SB1690CB AML cells was analyzed using multiple reaction monitoring-initiated detection and sequencing (MIDAS) (31). Following gel electrophoresis, the EVI1 containing band was excised and digested with trypsin. Peptides were separated by liquid chromatography prior to MIDAS using electrospray mass spectrometry on a 4000 Q-TRAP mass spectrometer (AB Sciex). MRM transitions were designed to detect 7–24 amino acid EVI1 peptides with serine, threonine or tyrosine phosphorylation within a Q1 *m/z* range from 400 to 1300 and in both a double and triple charge state. A Q3 mass of either 216.0 Da or Q1 minus 98 Da was used to identify tyrosine or serine/threonine phosphorylation, respectively. MS/MS data were interrogated using MASCOT and confirmed by manual inspection of spectra.

### Plasmids and site directed mutagenesis

The human EVI1 coding region was excised from pBABE-puro-flag-EVI1 (gift from Aubrey Thompson) (32) using Sall and EcoRI restriction sites and inserted into the Sall and EcoRI sites of pCMV-flag-5a. Substitution of S858 and S860 for alanine (A) to create the vector pCMV-EVI1-AQA-flag was done by site-directed mutagenesis using the QuikChange<sup>®</sup> II XL Kit (Agilent). The Codon-optimized mouse Evl1 lentiviral vector pRRL.PPT.SF.EVI1mCo.IRES\_EGFP.pre (19,33,34) was mutated as above to generate pRRL.PPT.SF.EVI1mCoAQA.IRES\_EGFP.pre. Control pRRL.PPT.SF.IRES\_EGFP.pre was generated by excision of the EVI1-ORF from pRRL.PPT.SF.EVI1mCo.IRES\_EGFP.pre vector with BamHI restriction enzyme and re-ligated to create an empty backbone vector. Lentiviral packaging vectors pHCMV-G, pMDLg/pRRE and pRSV-Rev were used as described (35). Primer sequences are provided in the Supplementary Table S3. Confirmation of mutated sequence is illustrated in Supplementary Figure S3.

### Gene expression analysis

Reporter gene assays were carried out in HEK293T cells as described before (details in Supplementary Material) (28), with RT-PCR monitored *EVI1*-expression (Supplementary Figure S4A). For Poly-A RNA sequencing (RNAseq) analysis of EVI1-mediated modulation of gene expression RNA was extracted from HEK293 cells, which were subjected to transient transfection using half confluent cultures with pCMV-flag, pCMV-EVI1-WT-flag or pCMV-EVI1-AQA-flag, exposed to 150  $\mu$ M H<sub>2</sub>O<sub>2</sub> or left untreated for 8 h. Equal levels of EVI1 levels were monitored by western blot (Supplementary Figure S4B). Libraries were prepared with the Lexogen QuantSeq 3' mRNA-Seq Library Prep Kit for Illumina (FWD) using an input of 200 ng and performing 14 cycles of amplification. Indexed libraries were then quantified using the Kapa Illumina Library quantification kit (Cat. 07960336001) and pooled. 1  $\times$  75 bp sequence reads were generated by clustering 2.0 pM of the library pool on a NextSeq500 High throughput run. Ordered BAM files were generated against the human genome feature file Homo\_sapiens.GRCh38.90.gtf downloaded from Ensembl (<ftp://ftp.ensembl.org/pub/current.gtf>) (36). Data analysis was performed using Qlucore Omics Explorer 3.3 (Qlucore, Lund, Sweden) with a FPKM (Fragments Per Kilobase Million) cut-off of 10. To identify significant differentially regulated transcripts, RNAseq expression data analysis was carried out by applying a group ANOVA with  $P < 0.01$  to the entire dataset. For illustration of the comparisons between the effect on transcription with EVI1-WT and EVI1-AQA in relation to untransfected cells and empty vector-transfected control cells with and without DNA damage, values were normalized to the mean of 0 and a variance of one. In addition, differences between expression levels at individual conditions were assessed by two group comparison ( $t$ -test). Biological pathways associated with differential gene expression were determined using a right-sided Fisher's exact test (Ingenuity Pathways Analysis, Qiagen). The effect on levels of expression detected by RNAseq were

confirmed by RT-PCR for selected transcripts using *taqman* technology with housekeeper transcripts (*YWHAZ* and  $\beta$ -*ACTIN*) chosen from a tested pool of housekeeper genes for minimal variation between samples and conditions (primer sequences and detailed methodology in supplementary material). RT-PCR data was processed for  $\Delta\Delta$ -CT calculation normalized to housekeeping transcripts.

### Rat-1 fibroblast transformation assay

Retroviral transduction of Rat-1 fibroblasts with human EVI1 was carried out as described previously (28), using FUGENHD (Promega)-transfected packaging Plat-E cells (MSCV-EVI1-IRES-GFP, MSCV-EVI1-AQA-IRES-GFP or empty vector control MSCV-IRES-GFP). After 4 days cells were FACS-sorted by GFP, and equal levels of EVI1 expression were confirmed by western blot (Supplementary Figure S5A–C). GFP<sup>+</sup> cells (10<sup>4</sup>) were seeded in untreated methylcellulose medium (MethoCult<sup>™</sup> M3231, Stem Cell Technology), or supplemented with 30  $\mu$ M of H<sub>2</sub>O<sub>2</sub>. Alternatively, 1  $\times$  10<sup>5</sup> cells in 100  $\mu$ l (96-well plate) were left untreated or irradiated (0.5 or 2 Gy). After 14 days, colony number and size were quantified and documented using a DMIL inverted microscope fitted with a MC170 HD camera (Leica) (Supplementary Figure S5D). Induction of DNA damage was assessed by induction of  $\gamma$ H2AX foci (Supplementary Figure S5E).

### Serial replating of hematopoietic progenitors

Hematopoietic c-Kit<sup>+</sup> progenitor cells were isolated from bone marrow of 8–10 week old C57/BL6 mice as previously described (28,37). Lentiviral mediated transduction was carried out with EVI1 vectors pRRL.PPT.SF.EVI1mCo.IRES\_EGFP.pre, and site mutated pRRL.PPT.SF.EVI1mCoAQA.IRES\_EGFP.pre as described (19,38). In brief, cells cultured in medium supplemented with 4  $\mu$ g/ml protamine (Sigma) were sequentially infected with two viral batches by spinoculation (60 min at 1250  $\times$   $g$  at 32°C), and cultured for two days in pre-stimulation serum free cytokine supplemented medium (StemCell Technologies), prior to FACS selection of GFP<sup>+</sup> cells. Equal transduction efficiency for EVI1-WT and EVI1-AQA was monitored by RT-PCR and quantitation of fluorescent signal (Supplementary Figures S6A and B). For replating 2  $\times$  10<sup>4</sup> GFP<sup>+</sup> cells were plated in cytokine supplemented Methocult M3231 medium, without and with H<sub>2</sub>O<sub>2</sub> at the prior demined IC<sub>50</sub> dose (30  $\mu$ M), with induction of genotoxic stress monitored by the induction of  $\gamma$ H2AX foci (Supplementary Figure S6C and D). After 7 days in culture, colonies were counted and morphologically assessed (Supplementary Figure S6E). Then cells were harvested, and 2  $\times$  10<sup>4</sup> cells were replated as before. Colonies were scored for subsequent rounds of replating as above, and previously H<sub>2</sub>O<sub>2</sub> treated colonies were split and either treated again or left untreated. For morphological assessment cytopsin preparations were stained with May-Grünwald Giemsa (Supplementary Figure S6F), and 200 cells per preparation were assessed.

## Immunofluorescence (IF)

For immunofluorescence cells were incubated with antibodies following standard procedures and image generation. Spatial association of EVI1 and CtBP1 was quantified by determining linear signal correlation by Pearson product-moment correlation coefficient (39) (further details in Supplementary Methods). Induction of the DNA damage response was confirmed by demonstration of increased frequency of  $\gamma$ H2AX foci (Supplementary Figure S7)

## RESULTS

### DNA damage mediates sequential phosphorylation of EVI1 on the carboxy-terminal SQS motif

To identify phosphorylation events on EVI1, we carried out a selective reaction monitoring mass spectrometric analysis of endogenously expressed EVI1 immunoprecipitated from EVI1-overexpressing SB1690CB AML cells. Under standard conditions we identified the HFIGNSNHGSQSPR (aa 849–862) peptide (NCBI accession: NP\_001098548.2) (Figure 1A). This peptide was also identified with a single site of phosphorylation (HFIGNSNHGSQpSPR), for which the MS/MS spectrum indicated serine phosphorylation at S860 (Figure 1B). This peptide involves an ATM (ataxia telangiectasia mutant)—kinase specific SQS motif (40), which is conserved across species (Figure 1C). We exposed cells to genotoxic stress by irradiation or H<sub>2</sub>O<sub>2</sub>, and confirmed induction of DNA damage by demonstration of increased  $\gamma$ H2AX foci and p53 phosphorylation (Figure 1D). Mass spectrometric analysis of immunoprecipitated EVI1 after DNA damage uncovered a doubly phosphorylated EVI1-peptide at residues S858 and S860 (Figure 1E). Western blot analysis of EVI1 using antibodies specifically raised against EVI1 peptides phosphorylated only at S860, or S858 plus S860 respectively, confirmed a rapid induction of doubly phosphorylated EVI1 both at S858 and S860 together after irradiation or H<sub>2</sub>O<sub>2</sub> treatment. This event was only detectable at very low levels in non-stressed cells, while correspondingly the signal for single phosphorylation at S860 decreased (Figure 2A). Pre-treatment with the ATM inhibitor KU55933 reduced the induction of the doubly phosphorylated (S858/S860) EVI1 after IR (Figure 2B). Mass spectrometric analysis of EVI1 repeatedly detected non-phosphorylated and EVI1 phosphorylated at S860 in untreated cells. After genotoxic stress EVI1 peptides with double phosphorylation at S858 and S860 were more abundant. However, a peptide indicating single phosphorylation on S858 alone was never detected. These findings suggest that the S858 phosphorylation is dynamically regulated in response to genotoxic stress after S860 phosphorylation.

### EVI1 transcriptional changes in the DNA damage response are sustained by carboxy-terminal SQS-phosphorylation

To functionally assess the carboxy-terminal SQS phosphorylation we generated site mutated EVI1 constructs to mimic non-phosphorylated, non-phosphorylatable EVI1 (EVI1-AQA), for comparison with the wild type EVI1-SQS (EVI1-WT) constructs. We first assessed target-gene promoter repression of EVI1-AQA compared with EVI1-WT and measured EVI1-mediated repression of *FOS* and *PLZF* (41,42).

EVI1-WT and EVI1-AQA mutant repressed *PLZF* promoter, regulated by the EVI1 N-terminal zinc-finger motif, and C-terminal zinc-finger motif regulated *FOS* promoter equally, indicating that EVI1 promoter repression was not affected by mutation of S858 and S860 (Figure 3A). We next compared the effect on transcriptional patterns mediated by EVI1-WT and EVI1-AQA. An RNAseq expression dataset was generated from untransfected, empty vector (vector-), EVI1-WT and EVI1-AQA transfected HEK293 cells, with and without DNA damage mediated by H<sub>2</sub>O<sub>2</sub>. We applied a group ANOVA with  $P < 0.01$  to the entire dataset and identified 1306 significantly differentially expressed transcripts (Supplementary Table S4, Sheet 1). Further detailed analysis of untreated EVI1-WT and EVI1-AQA compared to vector only transfected cells by two group comparison showed a strong overlap (Supplementary Table S4, Sheet 2): Of 62 significantly ( $P < 0.05$ ) up-regulated transcripts with EVI1-WT transfection compared to empty vector, 22 are also significantly up-regulated in EVI1-AQA transfected cells. Likewise, of 90 significantly repressed transcripts with EVI1-WT transfection, 30 are also significantly repressed in EVI1-AQA transfected cells. However, in the presence of damage, 10 of 41 upregulated transcripts in EVI1-WT transfected cells were also significantly upregulated in EVI1-AQA transfected cells, and of 47 repressed transcripts in EVI1-WT transfected cells, only 7 were also significantly repressed by EVI1-AQA transfection. Pathways affected by EVI1-WT transfection in the presence of genotoxic stress in this model included fucose-carbohydrate biosynthesis, death-receptor- and MAPK signaling (Supplementary Table S4, excel file, sheet 3). A heat map of 1306 the differentially expressed transcripts identified by group ANOVA when EVI1-WT and EVI1-AQA were compared with untransfected cells and empty vector control in untreated cells and with H<sub>2</sub>O<sub>2</sub> mediated DNA damage is clearly divided by vertical clustering in two halves by H<sub>2</sub>O<sub>2</sub>-induced genotoxic stress (Figure 3B). In untreated EVI1-transfected cells, horizontal dendrogram delineation separates two main clusters of EVI1-regulated transcripts, compared with non-transfected and vector-control transfected cells (boxed). In cluster 1, containing 139 transcripts, EVI1 mediated lower expression under normal conditions. For cluster 2, containing 328 transcripts, EVI1 mediated higher expression. Strikingly, when comparing heat-map patterns of untreated cells transfected with EVI1-WT with patterns from EVI1-AQA mutant transfected cells, the patterns boxed in cluster 1A and 2A are almost identical. Analysis in the same fashion of cells exposed to genotoxic stress by H<sub>2</sub>O<sub>2</sub> showed that EVI1-WT mediated expression changes are clustering and largely overlapping with those delineated in untreated cells. However, in the presence of genotoxic stress the expression patterns mediated by EVI1-WT compared to those mediated by EVI1-AQA are more diverse. In the cluster 1B a distinct sub-cluster of 14 transcripts is delineated with decreased expression in untreated EVI1-WT and EVI1-AQA transfected cells, but in response to damage are not repressed in the non-phosphorylatable EVI1-AQA (Figure 3B, arrow). In cluster 2B there are multiple transcripts that are higher expressed in untreated and damaged EVI1-WT transfected cells, but not in damaged EVI1-AQA transfected cells, which form a dis-

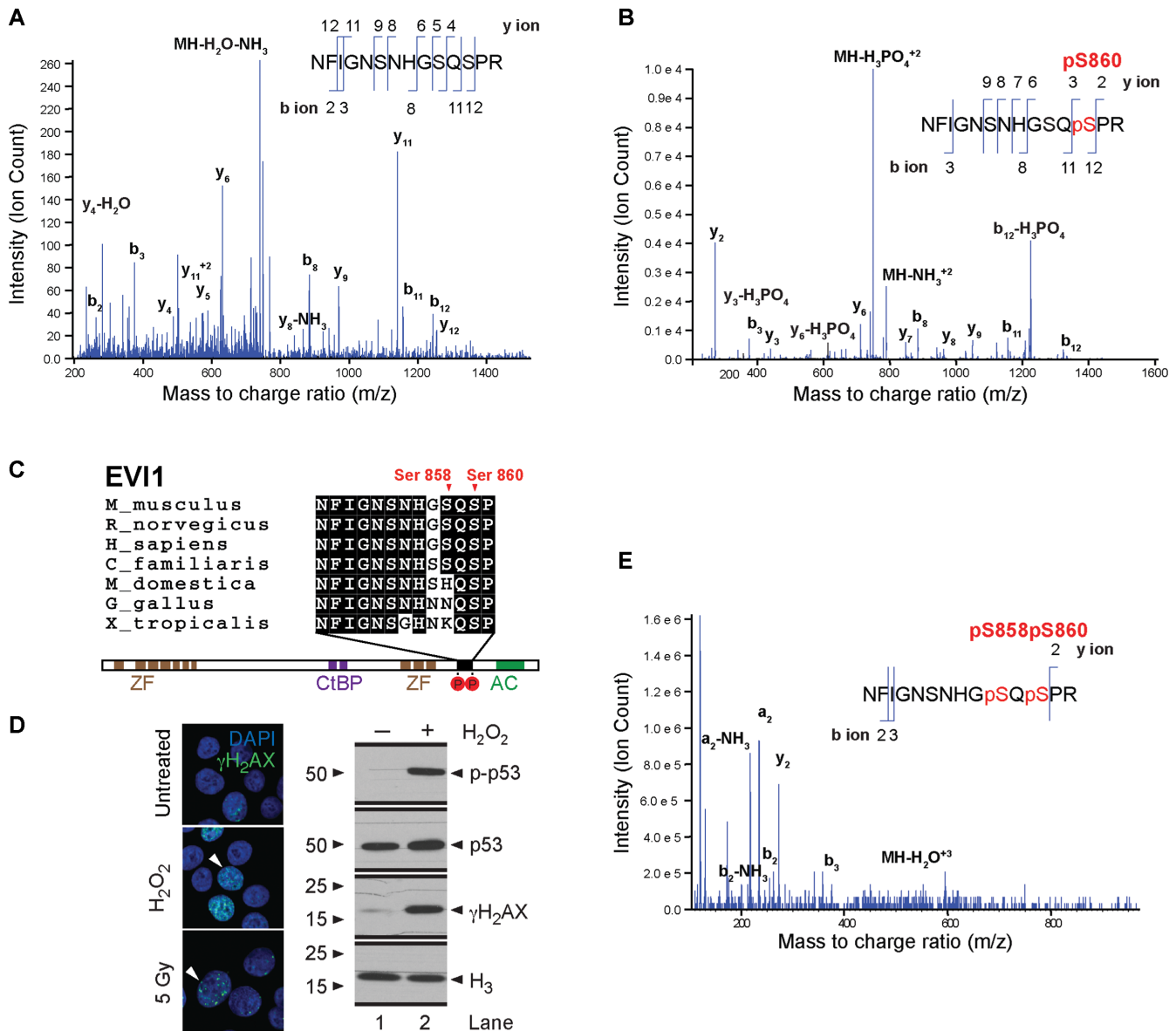


**Figure 1.** Carboxy-terminal EVI1 phosphorylation. Mass spectrometry analysis of the EVI1 peptide Asn849-Arg862 from SB1690CB AML cells, demonstrating the presence of non-phosphorylated (A) and single Ser860 phosphorylated peptides (B) in untreated SB1690CB cells. y- and b-type ions illustrating their position within the peptide sequence indicated. The mass/charge ratio (m/z) of the precursor ion is also shown. (C) Schematic representation of the EVI1 protein with sequence alignment of EVI1 from other species as indicated, showing DNA binding zinc finger domains (ZF), CtBP1 binding motifs (CtBP) and acidic domain (AC). Carboxy-terminal phosphorylation sites are shown in red circles and annotated in relation to the EVI1-SQS containing epitope alignment. (D) Confirmation of induction of DNA damage by  $\gamma$ H2AX foci formation after H<sub>2</sub>O<sub>2</sub> or radiation treatment of SB1690CB cells (left panel). White arrowheads denote cells with increased number of foci (green signal). DAPI co-stain for the nucleus (blue signal). Western blot (right panel) of  $\gamma$ H2AX and p-p53 (Ser15) as markers of DNA damage response activation and ATM activity after H<sub>2</sub>O<sub>2</sub>-treatment of SB1690CB cells. (E) EVI1 MS spectrum obtained for peptide Asn849-Arg862 from irradiated SB1690CB cells, inferring double phosphorylation of the carboxy-terminal S858/S860 SQS motif.

tinct sub-cluster of 93 transcripts (Figure 3B, dashed box). The modulatory effect on transcriptional patterns mediated by carboxy-terminal mutated EVI1-AQA is stronger in the presence of genotoxic stress.

### EVI1 carboxy-terminal phosphorylation sustains EVI1 transforming ability in the DNA damage response

To investigate to what extent the double phosphorylation at S858 and S860 also sustains EVI1-mediated transforma-

tion, we compared the effect of EVI1-WT with the EVI1-AQA mutant on Rat-1 fibroblast transformation (5). Equal expression of EVI1-WT and EVI1-AQA constructs in Rat-1 fibroblast cultures and activation of the DNA damage response in transduced cells was confirmed (Supplementary Figure 5A–E). Transduction with EVI1-WT resulted in a significant 2.2-fold (mean,  $n = 4$ ) increase in colony numbers after 14 days compared with vector only transduction, which under standard conditions was not significantly different from transduction with mutated EVI1-

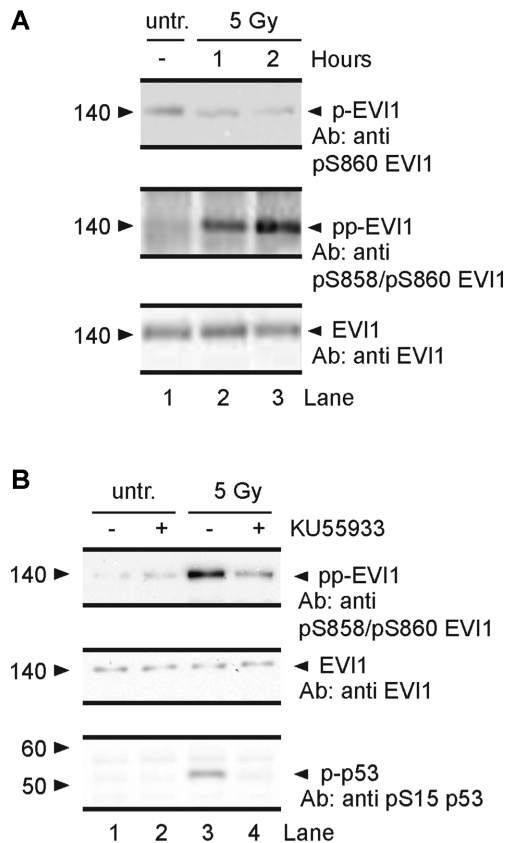


**Figure 2.** Induction of EVI1 double phosphorylation by DNA damage. (A) Immunoprecipitated EVI1 from SB1690CB cells probed with anti-pS860-EVI1 (upper panel), and anti-pS858/pS860-EVI1 antibody, untreated (lane 1), and after 1 and 2 h (lane 2 and 3) post radiation. (B) Western blot (WB) of EVI1-immunoprecipitates from untreated (lanes 1 and 2) and irradiated (lanes 3 and 4) SB1690CB cells pre-treated (1 h) with 10  $\mu$ M ATM-kinase inhibitor KU55933 (lanes 2 and 4), and not pre-treated (lanes 1 and 3). Membranes were probed for doubly phosphorylated EVI1 with anti-pS858/pS860-EVI1 antibody. Middle panel: membrane as upper panel re-probed with pan-EVI1 antibody. Lower panel: WB of p-p53 (Ser15) carried out on input samples as positive control for ATM-activity and ATM-inhibition.

AQA (Figure 4A). However, in the presence of genotoxic stress mediated by  $H_2O_2$ , EVI1-WT confers a 10.1-fold increase in colony numbers compared to vector only, while EVI1-AQA had a markedly weaker effect (Figure 4B). Radiation had a more profound effect on Rat-1 transformation. At 0.5 Gy EVI1-WT conferred doubling of colony numbers, while EVI1-AQA transduction did not significantly increase colony numbers compared with vector only. At 2 Gy only EVI1-WT conferred any significant increase in colony numbers compared to untransduced cells, while no significant increase in colony numbers was seen with EVI1-AQA transfection (Figure 4C).

#### The EVI1 carboxy-terminal SQS motif sustains hematopoietic self-renewal

Transduction with EVI1 has been shown to increase replating capacity of hematopoietic progenitor cells, reflecting the importance of EVI1 for hematopoietic self-renewal

(3,19). As ATM-knockout leads to haematopoietic stem cell exhaustion (43), we surmised that the ATM-mediated phosphorylation event at S858/S860 would be linked to EVI1-mediated self-renewal. We confirmed the replating potency of EVI1-WT with murine c-Kit<sup>+</sup> hematopoietic progenitor cells for three rounds of replating, untreated and in the presence of genotoxic stress (Figure 5A) ( $n = 8$ , from eight mice). Transduction with EVI1-AQA did not affect replating efficiency compared to EVI1-WT in the first round of plating (Figure 5B); vector only transfected cells also formed colonies. However, when replated in the second and third round, when vector only transfected cells did not form colonies, colony forming capacity of EVI1-AQA was significantly reduced compared with EVI1-WT (Figure 5C and D), even more profoundly in the presence of genotoxic stress. In line with these observations and published data (19), morphological analysis of EVI1-WT transduced colonies revealed a significant proportion of immature myeloid cells with blast-like morphology. Comparing EVI1-WT- with EVI1-AQA-transfected colonies uncovered a significantly reduced number of cells with blast-like morphology in EVI1-AQA transduced colonies even in the first round of replating (Figure 5E and F). These observations imply that maintenance of a hematopoietic blast-like and self-renewal phenotype by EVI1 is partly dependent on the phosphorylatable carboxy-terminal SQS motif.

#### Increased spatial association of EVI1 with CtBP1 in response to genotoxic stress

To explain the distinct effect of DNA damage induced phosphorylation on EVI1 transcription and transforming ability we hypothesized that these effects would be mediated by alteration of important EVI1 interactions with other transcriptionally active proteins. This seemed in particular plausible as the carboxy-terminal region has not been implicated in direct interaction of EVI1 with DNA, and SQS to AQA motif mutation had no effect on promoter repression (see above). As the interaction with the co-repressor CtBP1 is essential for EVI1-mediated transformation (22,27), and CtBP1 itself has a role in the maintenance of genomic integrity and DNA damage response (44,45), we investigated the effect of EVI1 carboxy-terminal phosphorylation, which does not directly involve the CtBP1 binding sites of EVI1 (27), on the EVI1-interaction with CtBP1 in the presence of genotoxic stress monitored by induction of  $\gamma$ H2AX foci (Supplementary Figure S7B and C). As the DNA damage response has been implicated in ATM-mediated phosphorylation determining cellular localization of proteins (40,46,47), we assessed the nuclear localization of EVI1 in relationship to CtBP1 with and without genotoxic stress. Under non-stressed conditions non-phosphorylatable mutant EVI1-AQA, which cannot be phosphorylated on this ATM consensus site, co-localized with CtBP1 in transfected HEK293T cells to the same degree as EVI1-WT. However, in the presence of genotoxic stress mediated by  $H_2O_2$  or radiation, we observed a highly significant increase in spatial association of EVI1-WT with CtBP1 of 22.1%  $\pm$  4.4 SEM with  $H_2O_2$  ( $n = 4$ ,  $P < 0.01$ ), and of 22.7%  $\pm$  2.4 SEM after radiation ( $P < 0.001$ ) (Figure 6A, upper two

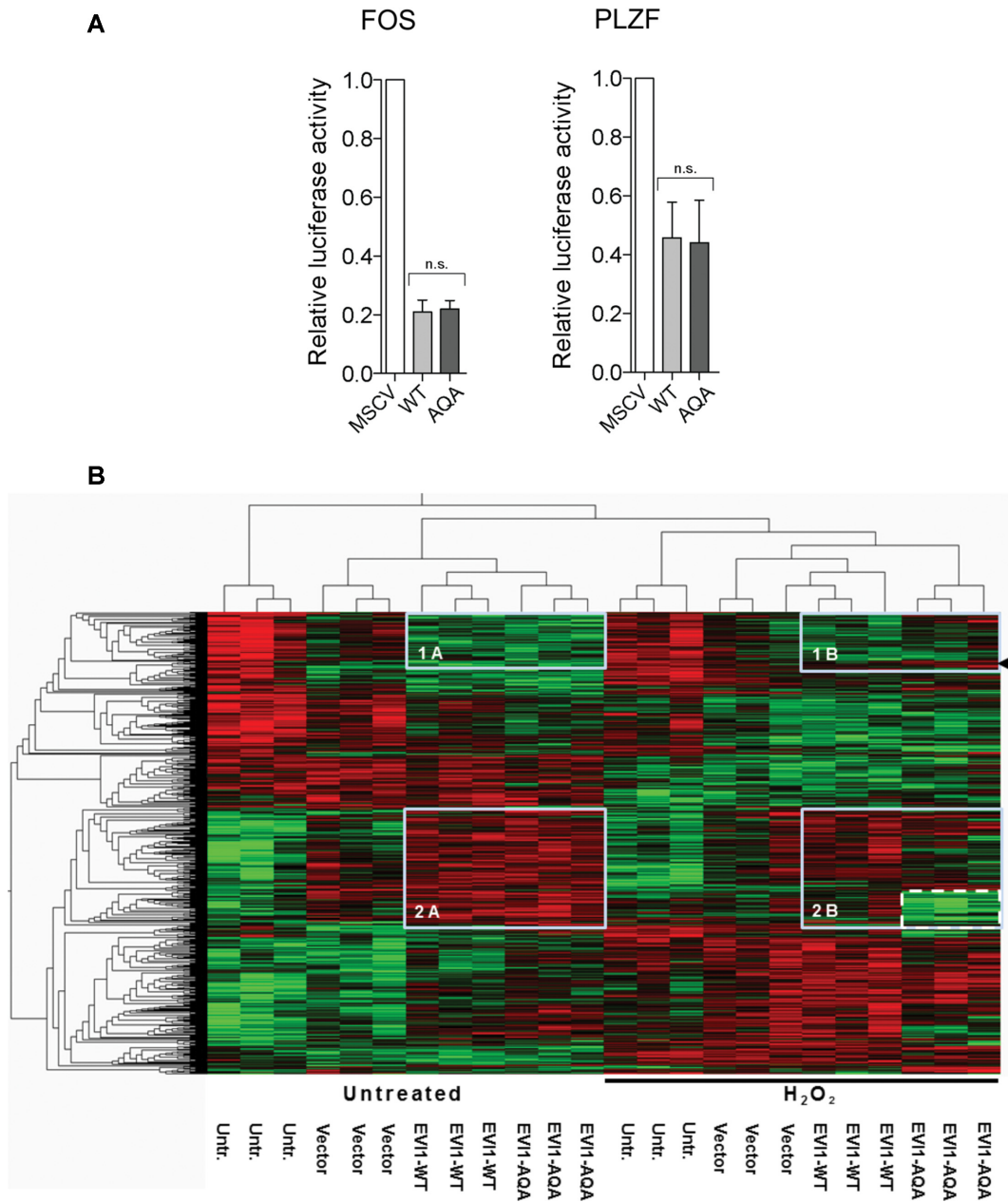


**Figure 3.** Effect of EVI1-WT and EVI1-AQA on transcription. (A) Luciferase assays on promoters of EVI1-repressed *PLZF* (left panel) and *FOS* (right panel) transcripts ( $n = 4$ ,  $t$ -test, ns: not significant). (B) Heat map illustration of significantly differentially expressed transcripts ( $P < 0.01$ ) after transfection with EVI1-WT and EVI1-AQA of untreated cells (left half of the heatmap), and after treatment with H<sub>2</sub>O<sub>2</sub> (150  $\mu$ M, right half of the heatmap, indicated by black line) ( $n = 1306$ ). The heatmap was generated applying a group ANOVA analysis to the entire dataset. Clusters of EVI1 regulated transcripts were identified by dendrogram delineation, and boxed for repressed (1A and 1B), and upregulated transcripts (2A and 2B). Patterns of sub-clusters in H<sub>2</sub>O<sub>2</sub> treated cells with different changes comparing EVI1-WT with EVI1-AQA indicated by arrow in 1B and dashed box in 2B.

panels and 6B). Non-phosphorylatable EVI1-AQA mutant failed to increase proximity in association with CtBP1 after treatment with H<sub>2</sub>O<sub>2</sub> or radiation. In endogenously EVI1-expressing SB1690CB AML cells, the highly significant increase in the degree of co-localization with CtBP1 in the presence of genotoxic stress was confirmed with cells with increases of  $18.7\% \pm 3.9$  SEM) after H<sub>2</sub>O<sub>2</sub> treatment, and  $24.9\% \pm 4.8$  SEM after radiation ( $n = 3$ ,  $P < 0.01$ ) (Figure 6A, lower panel, and C).

### Increased EVI1-CtBP1 interaction after genotoxic stress

In order to explore if the phosphorylation-mediated increase in co-localization of EVI1 with CtBP1 reflects EVI1 interaction, we performed co-immunoprecipitations using Flag-tagged EVI1-WT and EVI1-AQA in HEK293T cells. Comparing EVI1-WT with EVI1-AQA mutant, the levels of co-immunoprecipitated CtBP1 for EVI1-WT and EVI1-AQA mutant were not different under standard conditions (Figure 7A and B). However, the non-phosphorylatable

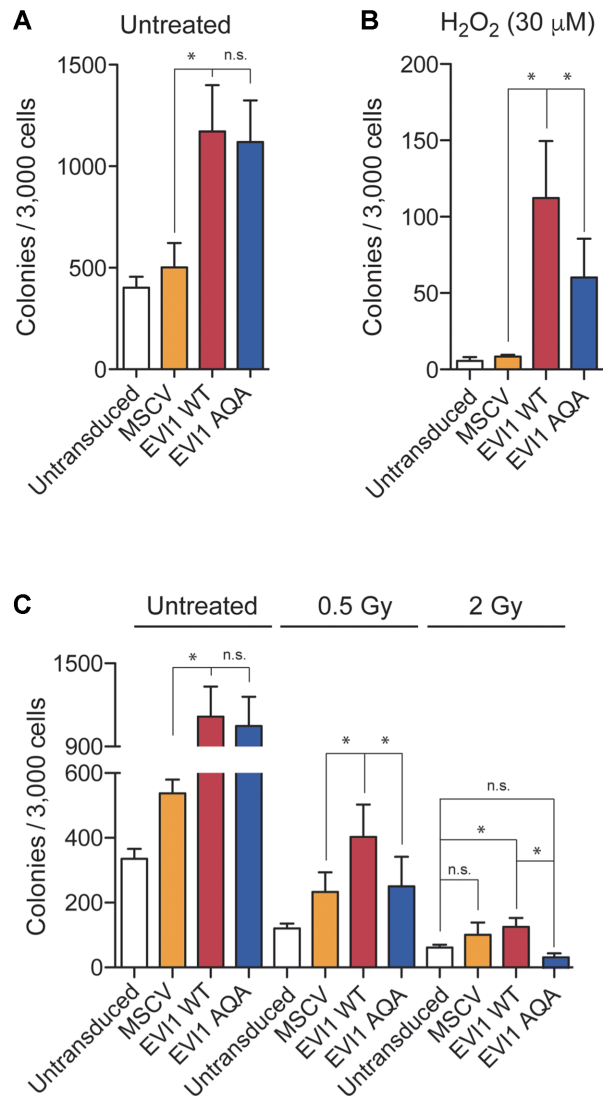


**Figure 4.** *EVI1*-mediated *Rat-1* fibroblast transformation. (A) *Rat-1* fibroblast colonies of untransduced, stably MSCV-, *EVI1*-WT- or *EVI1*-AQA-transduced fibroblasts. *Rat-1* fibroblasts were left untreated, H<sub>2</sub>O<sub>2</sub>-treated (B) or irradiated with 0.5 and 2Gy as indicated (C) ( $n = 4$ ). Statistical analysis: *t*-test (\* $P < 0.05$ , ns: not significant).

*EVI1*-AQA mutant showed  $36.9\% \pm 6.1$  SEM less co-immunoprecipitated CtBP1 ( $P < 0.05$ ) after treatment with H<sub>2</sub>O<sub>2</sub> compared with *EVI1*-WT (Figure 7C and D), implying greater *EVI1*-CtBP1 affinity after damage-mediated carboxyterminal *EVI1*-phosphorylation. Thus, the CtBP1-*EVI1* interaction in the DNA damage response is promoted by the carboxy-terminal *EVI1* phosphorylation, and points to the DNA damage response affecting transcriptionally relevant *EVI1* protein complex formations.

## DISCUSSION

*EVI1* is essential for early development, and further insight into *EVI1* function will help to define its role in maintenance of the stem cell phenotype. In view of the clinical relevance of aberrantly high expression of *EVI1* for malignant proliferation, better understanding of *EVI1*

functions will potentially also open novel therapeutic perspectives for *EVI1* overexpressing malignancies. Our mass spectrometry- and antibody-based analysis of *endogenously* expressed *EVI1* in SB1690CB AML cells confirms phosphorylation of the carboxy-terminal SQS site (S858 and S860). Carboxy-terminal phosphorylation of *EVI1* has previously been listed in global phosphoproteomic and targeted studies (29,40,48), but has not been further characterized or functionally assessed in any detail. We detected *EVI1* not phosphorylated at this motif, phosphorylated at S860, or doubly phosphorylated at S860 and S858 after induction of DNA damage. Building on previously published studies as above (29,40,48), our data imply that the S860 phosphorylation is likely to be present during normal cell proliferation, while the double phosphorylation on S860 and S858 is promoted via ATM, in particular in response to genotoxic stress. Reduction of the level of double phosphorylation with an ATM-inhibitor is in line with the recognition of the SQS-sequence as a specific ATM motif (40). Given the role of ATM in stem cell self-renewal (43), and *EVI1* for maintenance of the stem cell phenotype (1), we hypothesized a role of the carboxy-terminal SQS motif for this *EVI1* function, which we investigated by *EVI1* site directed mutagenesis and gene transfer. We first show that the modulatory effect mediated by *EVI1* on transcriptional patterns the presence genotoxic stress is dependent on the carboxy-terminal SQS motif. Aware of the limitations using the HEK293 model for investigating *EVI1*-target genes, we noted that known *EVI1*-affected transcripts such as *ALDOC* (18) were amongst significantly differentially expressed transcripts also in our model, and further investigations in respect of *EVI1*-modulated gene expression in particular in the presence of genotoxic stress, which in our model affected distinct cellular pathways, will be important to understand *EVI1*-mediated transcriptional modulation. In addition, in a clinical context modulation of *EVI1*-mediated gene expression by genotoxic stress and ATM, for example in response to chemotherapy, is likely to be relevant for gene expression patterns in *EVI1*-expressing leukaemia and solid tumors also in patient samples. We demonstrated the relevance of the carboxy-terminal SQS phosphorylation with respect to *EVI1*-mediated transformation using *Rat-1* fibroblasts, for which in the presence of genotoxic stress only phosphorylatable *EVI1*-WT sustains transformation, while *EVI1*-AQA lacking the ATM consensus site had reduced transforming ability. In murine haematopoietic progenitor cell replating, modelling the *EVI1*-function in early hematopoiesis, mutation of the carboxy-terminal ATM motif SQS to AQA significantly reduced re-plating capacity. ATM is required for the regulation of oxidative stress for self-renewal of hematopoietic cells (43), and *EVI1* expression is high in early haematopoietic cells (49). Thus, *EVI1* mediated hematopoietic self-renewal or maintenance capacity is likely linked by an ATM-*EVI1* axis, which is supported by the demonstration of reduced self-renewal mediated by *EVI1*-AQA, which lacks the ATM consensus site. But how is this achieved when mutation of the carboxy terminal SQS motif does affect DNA-binding and zinc finger motifs of *EVI1*, and does not alter gene promoter repression? We show that the *EVI1*-interaction with CtBP1 is dynamically and finely modulated by the ATM-mediated



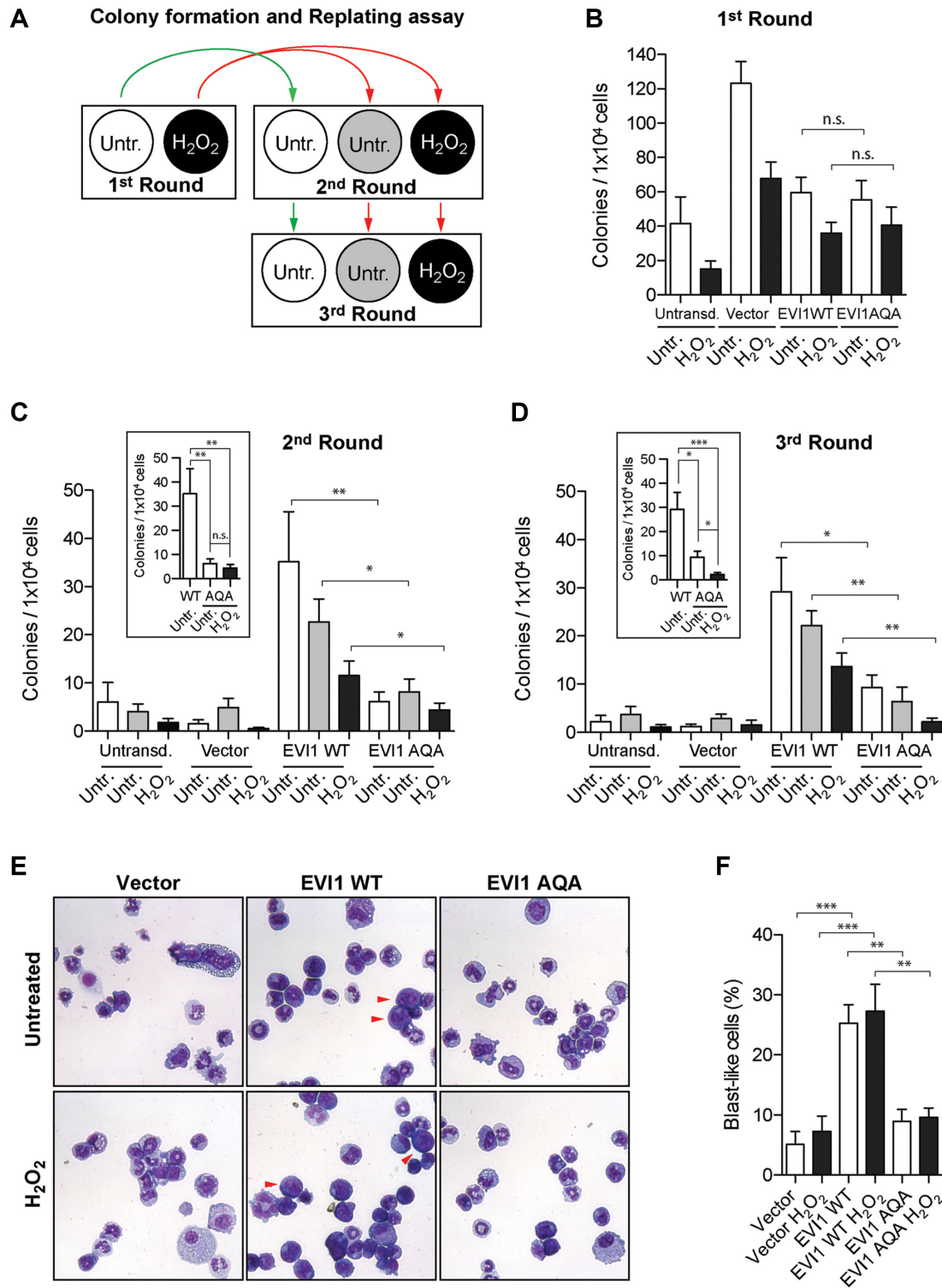


**Figure 5.** *EVI1*-mediated serial replating of murine hematopoietic progenitor cells. (A) Schematic representation of hematopoietic progenitor clonogenic replating: cKit<sup>+</sup> cells were transduced, selected for transduction, and plated in the presence or absence of H<sub>2</sub>O<sub>2</sub> (first round). Colonies were counted after 7 days, harvested and replated (second round). H<sub>2</sub>O<sub>2</sub> treated cells were split in two batches (red arrows) to be left untreated or treated with a second dose of H<sub>2</sub>O<sub>2</sub>. Untreated cells were re-plated untreated (green arrow). Remaining cells were used for a third round of replating. (B) Colony count after first round ( $n = 8$ , from eight different mice, black: H<sub>2</sub>O<sub>2</sub> treated). (C and D) Colony counts after the second and third rounds of replating ( $n = 8$ , from eight different mice). White: untreated; gray: untreated cells replated from previously H<sub>2</sub>O<sub>2</sub> treated colonies; black: H<sub>2</sub>O<sub>2</sub> treatment in all rounds. Inserts C and D: direct comparison between untreated *EVI1*-WT and *EVI1*-AQA transduction with and without damage. Statistical analysis: paired *t*-test (\* $P < 0.05$ , \*\* $P < 0.01$ ). (E) May-Grünwald Giemsa stained cells from colonies after first culture. Red arrowheads point typical blast-like cell morphology. (F) Blast-like cells quantitation from the first round of replating. Statistical analysis: one-way ANOVA (\*\* $P < 0.01$ , \*\*\* $P < 0.001$ ).

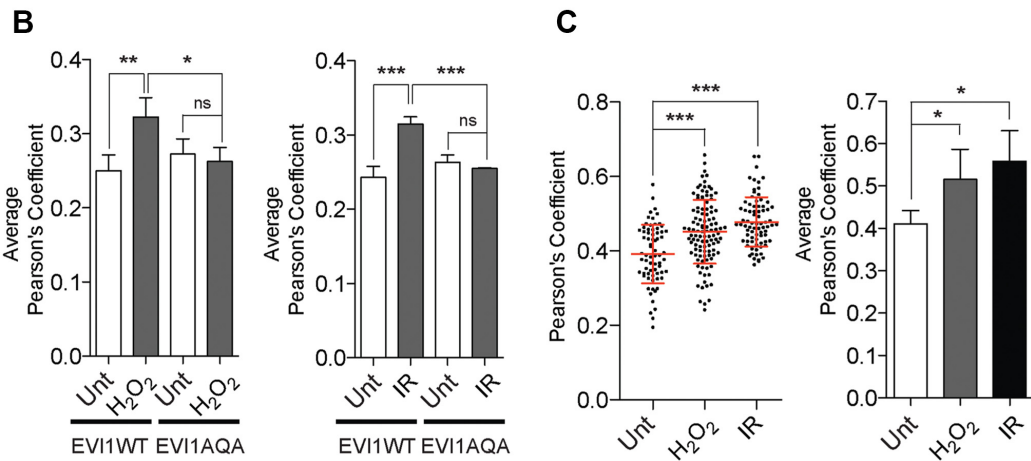
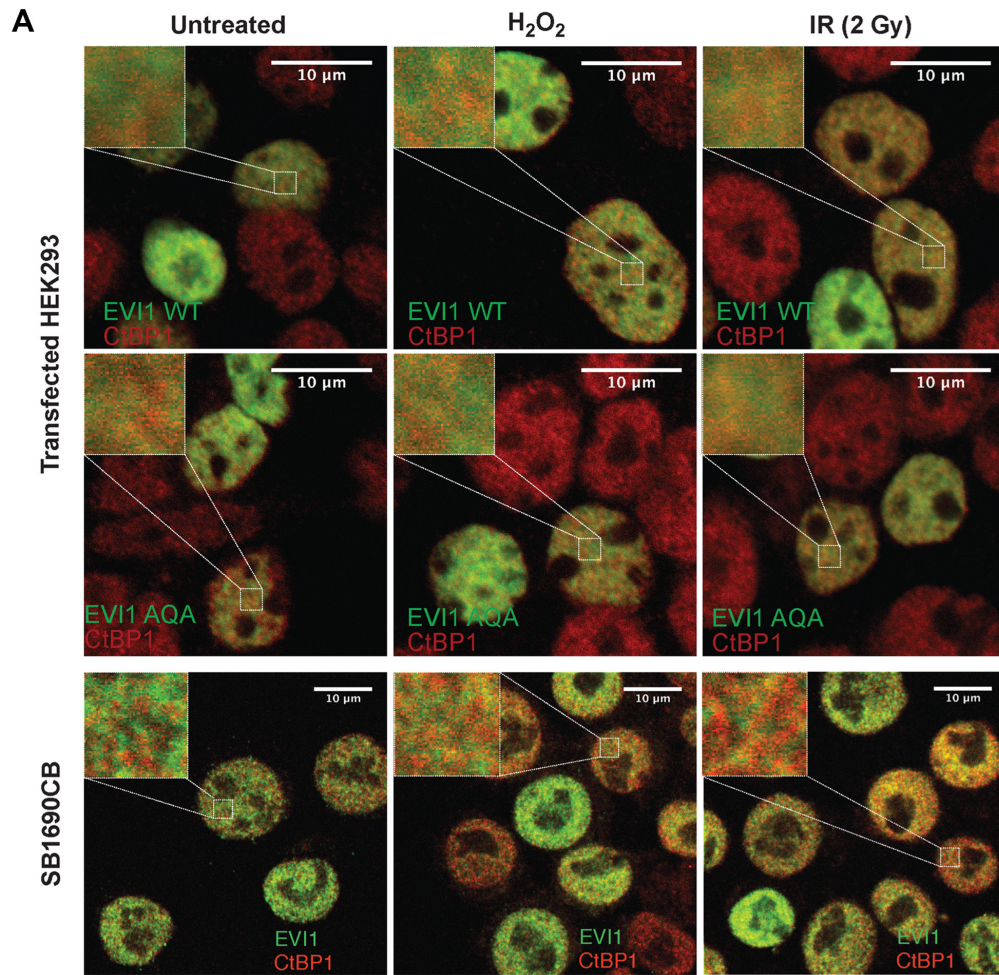


**Figure 6. Nuclear association of EVI1 with CtBP1.** (A) EVI1 (green) and CtBP1 (red) immunofluorescence signal of HEK293T cells transfected with EVI1-WT (upper panel) and EVI1-AQA mutant (middle panel), or SB1690CB AML cells (lower panel) after genotoxic stress induced either with H<sub>2</sub>O<sub>2</sub> treatment or irradiation (2 Gy). Left top corner inserts represent 4 μm<sup>2</sup> regions of interests (ROI) in HEK293T cells or 3 μm<sup>2</sup> ROIs in SB1690CB cells (eight ROIs/cell analyzed). (B) Quantification of EVI1 and CtBP1 co-localization in EVI1-WT or EVI1-AQA transfected HEK293T cells after genotoxic stress. Degree of co-localization is expressed as Pearson's Coefficient (P'sC). Each bar represents the average P'sC of independent experiments (n = 3) for H<sub>2</sub>O<sub>2</sub> (left panel) and irradiated cells (right panel). (C) Distribution of P'sC for endogenously expressed EVI1 and CtBP1 co-localization in SB1690CB leukemia cells after H<sub>2</sub>O<sub>2</sub> treatment or irradiation. Each dot represents a single cell (left panel). Average P'sC of independent experiments (n = 3) plotted as bar graphs (right panel). Statistical analysis: one-way ANOVA (\*P < 0.05, \*\*P < 0.01, \*\*\*P < 0.001, ns = not significant).

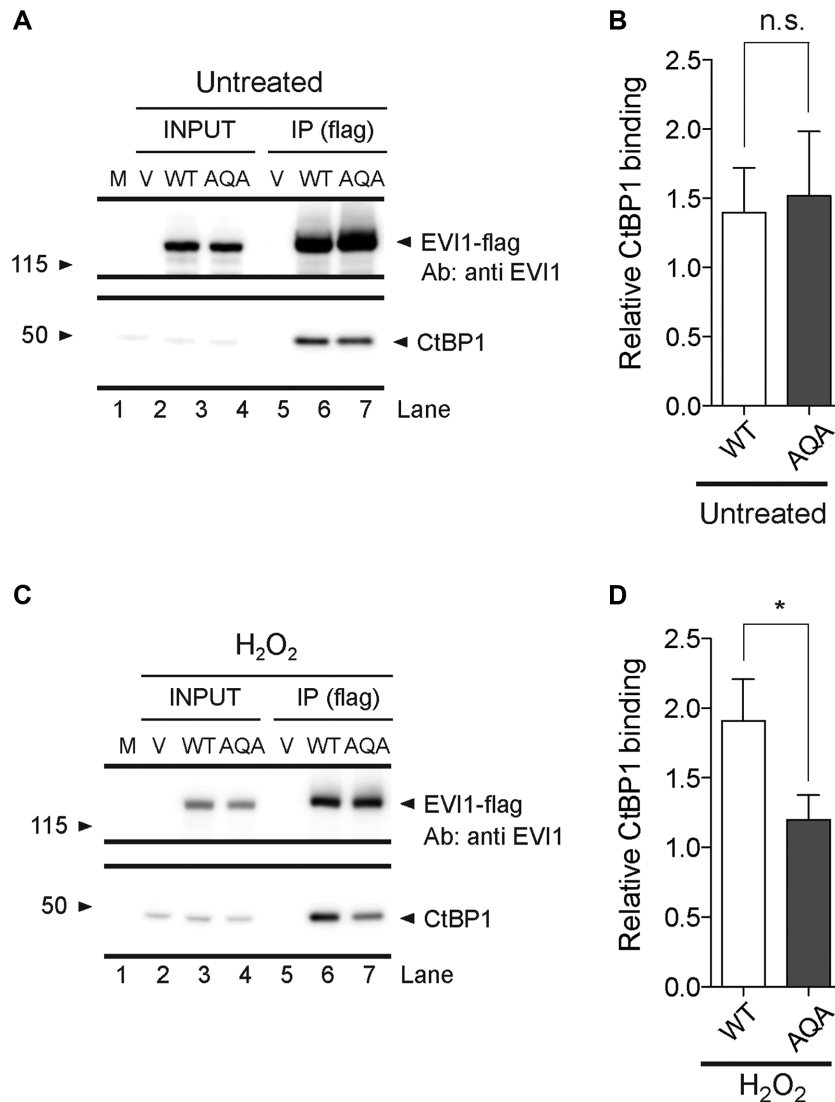


**Figure 7.** Effect of genotoxic stress on EVI1-CtBP1 interaction. (A) Western blot analysis of flag-antibody immunoprecipitated tagged EVI1 and co-immunoprecipitated CtBP1 from total cell protein extracts of untreated Flag-tagged EVI1-WT or EVI1-AQA transfected HEK293 cells (upper panel: EVI1; lower panel: CtBP1). (B) Signal quantification of serial biological replicates ( $n = 3$ ) at 3 min (n.s. = not significant,  $t$ -test). (C) Western blot analysis of flag-antibody immunoprecipitated EVI1 and co-immunoprecipitated CtBP1 from total cell protein extracts of H<sub>2</sub>O<sub>2</sub> treated Flag-tagged EVI1-WT and EVI1-AQA transfected cells (upper panel: EVI1; lower panel CtBP1). (D) Signal quantification of biological replicates ( $n = 3$ ) ( $*P < 0.05$ ,  $t$ -test).

EVI1-SQS phosphorylation and enhanced by genotoxic stress. The interaction with CtBP1 is essential for EVI1 function with respect to transformation and leukaemogenesis in murine haematopoietic progenitor cells (27,50), and modulated by ATM without directly affecting previously described CtBP1 binding regions, which involve amino acids 553–559 and 584–590 (27). This might involve charge-mediated affinity between proteins, altered tertiary structure, or posttranslational modification of CtBP1 or other proteins, which we are investigating. Data presented here support a concept by which EVI1 phosphorylation links ATM and the DNA damage response to essential EVI1 protein interactions for transcriptional regulation, transformation and self-renewal. This novel aspect of EVI1 function, in particular with respect to transformation and self-renewal, is therapeutically relevant for EVI1-overexpressing

malignancies, as chemotherapy induced genotoxicity might detrimentally sustain EVI1 function. Inhibition of ATM with an orally applicable compound (51) is currently subject to phase 1 clinical evaluation and has shown activity in a murine leukaemia model (52). ATM inhibition or therapeutic interference of the enhanced EVI1 interaction with CtBP1 after genotoxic stress might be of particular benefit in EVI1 overexpressing malignancies, and this will be subject to further work.

#### DATA AVAILABILITY

Gene expression data from RNAseq experiments are available on GEO (submission No GSE115643).

## SUPPLEMENTARY DATA

Supplementary Data are available at NAR Online.

## FUNDING

Bloodwise [10037, 150380]; Cancer Research UK [C5759/A20971, C18601/A5901]; The Kay Kendall Leukemia Fund [KKL 792], Children with Cancer, UK; The Elimination of Leukaemia Fund, UK; The UK Children's Cancer and Leukaemia Group (CCLG GA201609, Toti Worboys Leukaemia Project Grant to J.R.K.); The Ogelsby Leukaemia Research Fellowship to DHW, The Medical Research Council (Grant No MR/M008959/1), UK; Deutsche Forschungsgemeinschaft (Cluster of Excellence REBIRTH) [EXC 62/1]. Funding for open access charge: Institutional support and grant budget.

*Conflict of interest statement.* HvdV is a founding member of New Haven Biosciences Consulting.

## REFERENCES

- Goyama, S., Yamamoto, G., Shimabe, M., Sato, T., Ichikawa, M., Ogawa, S., Chiba, S. and Kurokawa, M. (2008) Evi-1 is a critical regulator for hematopoietic stem cells and transformed leukemic cells. *Cell Stem Cell*, **3**, 207–220.
- Konantz, M., Alghisi, E., Muller, J.S., Lenard, A., Esain, V., Carroll, K.J., Kanz, L., North, T.E. and Lengerke, C. (2016) Evi1 regulates Notch activation to induce zebrafish hematopoietic stem cell emergence. *EMBO J.*, **35**, 2315–2331.
- Kataoka, K., Sato, T., Yoshimi, A., Goyama, S., Tsuruta, T., Kobayashi, H., Shimabe, M., Arai, S., Nakagawa, M., Imai, Y. *et al.* (2011) Evi1 is essential for hematopoietic stem cell self-renewal, and its expression marks hematopoietic cells with long-term multilineage repopulating activity. *J. Exp. Med.*, **208**, 2403–2416.
- Buonamici, S., Li, D., Chi, Y., Zhao, R., Wang, X., Brace, L., Ni, H., Sauntharajah, Y. and Nucifora, G. (2004) EVI1 induces myelodysplastic syndrome in mice. *J. Clin. Invest.*, **114**, 713–719.
- Bartholomew, C., Kilbey, A., Clark, A.M. and Walker, M. (1997) The Evi-1 proto-oncogene encodes a transcriptional repressor activity associated with transformation. *Oncogene*, **14**, 569–577.
- Groschel, S., Lugthart, S., Schlenk, R.F., Valk, P.J., Eiwien, K., Goudswaard, C., van Putten, W.J., Kayser, S., Verdonck, L.F., Lubbert, M. *et al.* (2010) High EVI1 expression predicts outcome in younger adult patients with acute myeloid leukemia and is associated with distinct cytogenetic abnormalities. *J. Clin. Oncol.*, **28**, 2101–2107.
- Lugthart, S., van Drunen, E., van Norden, Y., van Hoven, A., Erpelinck, C.A., Valk, P.J., Beverloo, H.B., Lowenberg, B. and Delwel, R. (2008) High EVI1 levels predict adverse outcome in acute myeloid leukemia: prevalence of EVI1 overexpression and chromosome 3q26 abnormalities underestimated. *Blood*, **111**, 4329–4337.
- Stein, S., Ott, M.G., Schultze-Strasser, S., Jauch, A., Burwinkel, B., Kinner, A., Schmidt, M., Kramer, A., Schwable, J., Glimm, H. *et al.* (2010) Genomic instability and myelodysplasia with monosomy 7 consequent to EVI1 activation after gene therapy for chronic granulomatous disease. *Nat. Med.*, **16**, 198–204.
- Meyer, S., Bristow, C., Wappett, M., Pepper, S., Whetton, A.D., Hanenberg, H., Neitzel, H., Wlodarski, M.W., Ebell, W., Tönnies, H. *et al.* (2011) Fanconi anemia (FA)-associated 3q gains in leukemic transformation consistently target EVI1, but do not affect low TERC expression in FA. *Blood*, **117**, 6047–6050.
- Meyer, S., Fergusson, W.D., Whetton, A.D., Moreira-Leite, F., Pepper, S.D., Miller, C., Saunders, E.K., White, D.J., Will, A.M., Eden, T. *et al.* (2007) Amplification and translocation of 3q26 with overexpression of EVI1 in Fanconi anemia-derived childhood acute myeloid leukemia with biallelic FANCD1/BRCA2 disruption. *Genes Chromosomes Cancer*, **46**, 359–372.
- Dutta, P., Bui, T., Bauckman, K.A., Keyomarsi, K., Mills, G.B. and Nanjundan, M. (2013) EVI1 splice variants modulate functional responses in ovarian cancer cells. *Mol. Oncol.*, **7**, 647–668.
- Koos, B., Bender, S., Witt, H., Mertsch, S., Felsberg, J., Beschoner, R., Korshunov, A., Riesmeier, B., Pfister, S., Paulus, W. *et al.* (2011) The transcription factor evi-1 is overexpressed, promotes proliferation, and is prognostically unfavorable in infratentorial ependymomas. *Clin. Cancer Res.*, **17**, 3631–3637.
- Wang, H., Schaefer, T., Konantz, M., Braun, M., Varga, Z., Paczulla, A.M., Reich, S., Jacob, F., Perner, S., Moch, H. *et al.* (2017) Prominent oncogenic roles of EVI1 in breast carcinoma. *Cancer Res.*, **77**, 2148–2160.
- Queisser, A., Hagedorn, S., Wang, H., Schaefer, T., Konantz, M., Alavi, S., Deng, M., Vogel, W., von Massenhausen, A., Kristiansen, G. *et al.* (2017) Ecotropic viral integration site 1, a novel oncogene in prostate cancer. *Oncogene*, **36**, 1573–1584.
- Krivtsov, A.V., Figueroa, M.E., Sinha, A.U., Stubbs, M.C., Feng, Z., Valk, P.J., Delwel, R., Dohner, K., Bullinger, L., Kung, A.L. *et al.* (2013) Cell of origin determines clinically relevant subtypes of MLL-rearranged AML. *Leukemia*, **27**, 852–860.
- Regha, K., Assi, S.A., Toulaki, O., Gilmour, J., Lacaud, G. and Bonifer, C. (2015) Developmental-stage-dependent transcriptional response to leukaemic oncogene expression. *Nat. Commun.*, **6**, 7203.
- Stevens, A., Hanson, D., de Leonibus, C., Whatmore, A., Donn, R., White, D.J., Liu, J., van den Heuvel-Eibrink, M.M., Saha, V., Clayton, P.E. *et al.* (2014) EVI1 expression in childhood acute lymphoblastic leukaemia is not restricted to MLL and BCR/ABL rearrangements and is influenced by age. *Blood Cancer J.*, **4**, e179.
- Fenouille, N., Bassil, C.F., Ben-Sahra, I., Benajiba, L., Alexe, G., Ramos, A., Pikman, Y., Conway, A.S., Burgess, M.R., Li, Q. *et al.* (2017) The creatine kinase pathway is a metabolic vulnerability in EVI1-positive acute myeloid leukemia. *Nat. Med.*, **23**, 301–313.
- Kustikova, O.S., Schwarzer, A., Stahlhut, M., Brugman, M.H., Neumann, T., Yang, M., Li, Z., Schambach, A., Heinz, N., Gerdes, S. *et al.* (2013) Activation of Evi1 inhibits cell cycle progression and differentiation of hematopoietic progenitor cells. *Leukemia*, **27**, 1127–1138.
- Delwel, R., Funabiki, T., Kreider, B.L., Morishita, K. and Ihle, J.N. (1993) Four of the seven zinc fingers of the Evi-1 myeloid transforming gene are required for sequence-specific binding to GA(C/T)AAGA(T/C)AAGATAA. *Mol. Cell. Biol.*, **13**, 4291–4300.
- Funabiki, T., Kreider, B.L. and Ihle, J.N. (1994) The carboxyl domain of zinc fingers of the Evi-1 myeloid transforming gene binds a consensus sequence of GAAGATGAG. *Oncogene*, **9**, 1575–1581.
- Izutsu, K., Kurokawa, M., Imai, Y., Maki, K., Mitani, K. and Hirai, H. (2001) The corepressor CtBP interacts with Evi-1 to repress transforming growth factor beta signaling. *Blood*, **97**, 2815–2822.
- Goyama, S., Nitta, E., Yoshino, T., Kako, S., Watanabe-Okochi, N., Shimabe, M., Imai, Y., Takahashi, K. and Kurokawa, M. (2010) EVI-1 interacts with histone methyltransferases SUV39H1 and G9a for transcriptional repression and bone marrow immortalization. *Leukemia*, **24**, 81–88.
- Chi, Y., Senyuk, V., Chakraborty, S. and Nucifora, G. (2003) EVI1 promotes cell proliferation by interacting with BRG1 and blocking the repression of BRG1 on E2F1 activity. *J. Biol. Chem.*, **278**, 49806–49811.
- Yoshimi, A., Goyama, S., Watanabe-Okochi, N., Yoshiki, Y., Nannya, Y., Nitta, E., Arai, S., Sato, T., Shimabe, M., Nakagawa, M. *et al.* (2011) Evi1 represses PTEN expression and activates PI3K/AKT/mTOR via interactions with polycomb proteins. *Blood*, **117**, 3617–3628.
- Nitta, E., Izutsu, K., Yamaguchi, Y., Imai, Y., Ogawa, S., Chiba, S., Kurokawa, M. and Hirai, H. (2005) Oligomerization of Evi-1 regulated by the PR domain contributes to recruitment of corepressor CtBP. *Oncogene*, **24**, 6165–6173.
- Palmer, S., Brouillet, J.P., Kilbey, A., Fulton, R., Walker, M., Crossley, M. and Bartholomew, C. (2001) Evi-1 transforming and repressor activities are mediated by CtBP co-repressor proteins. *J. Biol. Chem.*, **276**, 25834–25840.
- White, D.J., Unwin, R.D., Bindels, E., Pierce, A., Teng, H.Y., Muter, J., Greystoke, B., Somerville, T.D., Griffiths, J., Lovell, S. *et al.* (2013) Phosphorylation of the leukemic oncoprotein EVI1 on serine 196

- modulates DNA binding, transcriptional repression and transforming ability. *PLoS One*, **8**, e66510.
29. Bard-Chapeau, E.A., Gunaratne, J., Kumar, P., Chua, B.Q., Muller, J., Bard, F.A., Blackstock, W., Copeland, N.G. and Jenkins, N.A. (2013) EVI1 oncoprotein interacts with a large and complex network of proteins and integrates signals through protein phosphorylation. *Proc. Natl. Acad. Sci. U.S.A.*, **110**, E2885–E2894.
  30. Gulden, M., Jess, A., Kammann, J., Maser, E. and Seibert, H. (2010) Cytotoxic potency of H<sub>2</sub>O<sub>2</sub> in cell cultures: impact of cell concentration and exposure time. *Free Rad. Biol. Med.*, **49**, 1298–1305.
  31. Unwin, R.D., Griffiths, J.R., Leverenz, M.K., Grallert, A., Hagan, I.M. and Whetton, A.D. (2005) Multiple reaction monitoring to identify sites of protein phosphorylation with high sensitivity. *Mol. Cell. Proteomics: MCP*, **4**, 1134–1144.
  32. Liu, Y., Chen, L., Ko, T.C., Fields, A.P. and Thompson, E.A. (2006) Evi1 is a survival factor which conveys resistance to both TGFβ and taxol-mediated cell death via PI3K/AKT. *Oncogene*, **25**, 3565–3575.
  33. Konantz, M., Andre, M.C., Ebinger, M., Grauer, M., Wang, H., Grzywna, S., Rothfuss, O.C., Lehle, S., Kustikova, O.S., Salihi, H.R. *et al.* (2013) EVI-1 modulates leukemogenic potential and apoptosis sensitivity in human acute lymphoblastic leukemia. *Leukemia*, **27**, 56–65.
  34. Schambach, A., Bohne, J., Chandra, S., Will, E., Margison, G.P., Williams, D.A. and Baum, C. (2006) Equal potency of gammaretroviral and lentiviral SIN vectors for expression of O<sub>6</sub>-methylguanine-DNA methyltransferase in hematopoietic cells. *Mol. Ther.*, **13**, 391–400.
  35. Ding, X., Ray Chaudhuri, A., Callen, E., Pang, Y., Biswas, K., Klarmann, K.D., Martin, B.K., Burkett, S., Cleveland, L., Stauffer, S. *et al.* (2016) Synthetic viability by BRCA2 and PARP1/ARTD1 deficiencies. *Nat. Commun.*, **7**, 12425.
  36. Aken, B.L., Achuthan, P., Akanni, W., Amode, M.R., Bernsdorff, F., Bhai, J., Billis, K., Carvalho-Silva, D., Cummins, C., Clapham, P. *et al.* (2017) Ensembl 2017. *Nucleic Acids Res.*, **45**, D635–D642.
  37. Somervaille, T.C., Matheny, C.J., Spencer, G.J., Iwasaki, M., Rinn, J.L., Witten, D.M., Chang, H.Y., Shurtleff, S.A., Downing, J.R. and Cleary, M.L. (2009) Hierarchical maintenance of MLL myeloid leukemia stem cells employs a transcriptional program shared with embryonic rather than adult stem cells. *Cell Stem Cell*, **4**, 129–140.
  38. Cante-Barrett, K., Mendes, R.D., Smits, W.K., van Helsingingen-van Wijk, Y.M., Pieters, R. and Meijerink, J.P. (2016) Lentiviral gene transfer into human and murine hematopoietic stem cells: size matters. *BMC Res. Notes*, **9**, 312.
  39. Dunn, K.W., Kamocka, M.M. and McDonald, J.H. (2011) A practical guide to evaluating colocalization in biological microscopy. *Am. J. Physiol. Cell Physiol.*, **300**, C723–C742.
  40. Matsuoka, S., Ballif, B.A., Smogorzewska, A., McDonald, E.R. 3rd, Hurov, K.E., Luo, J., Bakalarski, C.E., Zhao, Z., Solimini, N., Lerenthal, Y. *et al.* (2007) ATM and ATR substrate analysis reveals extensive protein networks responsive to DNA damage. *Science*, **316**, 1160–1166.
  41. Bard-Chapeau, E.A., Jeyakani, J., Kok, C.H., Muller, J., Chua, B.Q., Gunaratne, J., Batagov, A., Jenjaroenpun, P., Kuznetsov, V.A., Wei, C.L. *et al.* (2012) Ecotopic viral integration site 1 (EVI1) regulates multiple cellular processes important for cancer and is a synergistic partner for FOS protein in invasive tumors. *Proc. Natl. Acad. Sci. U.S.A.*, **109**, 2168–2173.
  42. Takahashi, S. and Licht, J.D. (2002) The human promyelocytic leukemia zinc finger gene is regulated by the Evi-1 oncoprotein and a novel guanine-rich site binding protein. *Leukemia*, **16**, 1755–1762.
  43. Ito, K., Hirao, A., Arai, F., Matsuoka, S., Takubo, K., Hamaguchi, I., Nomiyama, K., Hosokawa, K., Sakurada, K., Nakagata, N. *et al.* (2004) Regulation of oxidative stress by ATM is required for self-renewal of haematopoietic stem cells. *Nature*, **431**, 997–1002.
  44. Chinnadurai, G. (2009) The transcriptional corepressor CtBP: a foe of multiple tumor suppressors. *Cancer Res.*, **69**, 731–734.
  45. Di, L.J., Byun, J.S., Wong, M.M., Wakano, C., Taylor, T., Bilke, S., Baek, S., Hunter, K., Yang, H., Lee, M. *et al.* (2013) Genome-wide profiles of CtBP link metabolism with genome stability and epithelial reprogramming in breast cancer. *Nat. Commun.*, **4**, 1449.
  46. Jeyasekharan, A.D., Ayoub, N., Mahen, R., Ries, J., Esposito, A., Rajendra, E., Hattori, H., Kulkarni, R.P. and Venkitaraman, A.R. (2010) DNA damage regulates the mobility of Brca2 within the nucleoplasm of living cells. *Proc. Natl. Acad. Sci. U.S.A.*, **107**, 21937–21942.
  47. Reuter, M., Zelensky, A., Smal, I., Meijering, E., van Cappellen, W.A., de Gruiter, H.M., van Belle, G.J., van Royen, M.E., Houtsmuller, A.B., Essers, J. *et al.* (2015) BRCA2 diffuses as oligomeric clusters with RAD51 and changes mobility after DNA damage in live cells. *J. Cell Biol.*, **208**, 857.
  48. Olsen, J.V., Blagoev, B., Gnäd, F., Macek, B., Kumar, C., Mortensen, P. and Mann, M. (2006) Global, in vivo, and site-specific phosphorylation dynamics in signaling networks. *Cell*, **127**, 635–648.
  49. Cabezas-Wallscheid, N., Klimmeck, D., Hansson, J., Lipka, D.B., Reyes, A., Wang, Q., Weichenhan, D., Lier, A., von Paleske, L., Renders, S. *et al.* (2014) Identification of regulatory networks in HSCs and their immediate progeny via integrated proteome, transcriptome, and DNA methylome analysis. *Cell Stem Cell*, **15**, 507–522.
  50. Senyuk, V., Chakraborty, S., Mikhail, F.M., Zhao, R., Chi, Y. and Nucifora, G. (2002) The leukemia-associated transcription repressor AML1/MDS1/EVI1 requires CtBP to induce abnormal growth and differentiation of murine hematopoietic cells. *Oncogene*, **21**, 3232–3240.
  51. Pike, K.G., Barlaam, B., Cadogan, E., Campbell, A., Chen, Y., Colclough, N., Davies, N.L., DeAlmeida, C., Degorce, S.L., Didelot, M. *et al.* (2018) The identification of potent, selective and orally available inhibitors of ataxia telangiectasia mutated (ATM) Kinase: The discovery of AZD0156 (8-{6-[3-(dimethylamino)propoxy]pyridin-3-yl}-3-methyl-1-(tetrahydro-2H-pyran-4-yl)-1,3-dihydro-2H-imidazo[4,5-c]quinolin-2-one). *J. Med. Chem.*, **61**, 3823–3841.
  52. Morgado-Palacin, I., Day, A., Murga, M., Lafarga, V., Anton, M.E., Tubbs, A., Chen, H.T., Ergan, A., Anderson, R., Bhandoola, A. *et al.* (2016) Targeting the kinase activities of ATR and ATM exhibits antitumoral activity in mouse models of MLL-rearranged AML. *Sci. Signal.*, **9**, ra91.